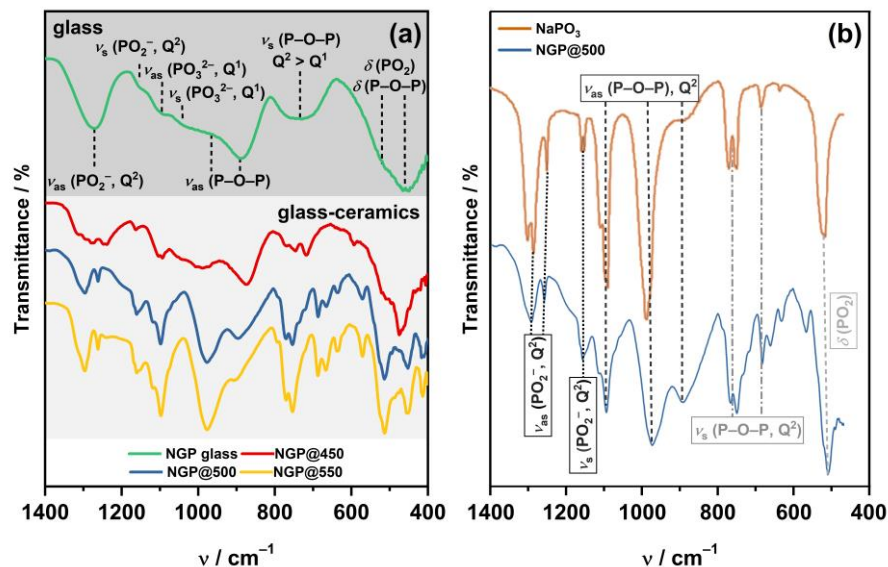


# The Crystallization Behavior of a Na<sub>2</sub>O-GeO<sub>2</sub>-P<sub>2</sub>O<sub>5</sub> Glass System: A (Micro)Structural, Electrical, and Dielectric Study

Sara Marijan <sup>1</sup>, Marta Razum <sup>1</sup>, Kristina Sklepić Kerhač <sup>1</sup>, Petr Mošner <sup>2</sup>, Ladislav Koudelka <sup>2</sup>, Jana Pisk <sup>3</sup>, Andrea Moguš-Milanković <sup>1</sup>, Željko Skoko <sup>4,\*</sup> and Luka Pavić <sup>1,\*</sup>

- <sup>1</sup> Division of Materials Chemistry, Ruđer Bošković Institute, Bijenička 54, 10000 Zagreb, Croatia; smarijan@irb.hr (S.M.); mrazum@irb.hr (M.R.); ksklepickerhac@gmail.com (K.S.K.); mogus@irb.hr (A.M.-M.)
  - <sup>2</sup> Department of General and Inorganic Chemistry, Faculty of Chemical Technology, University of Pardubice, 53210 Pardubice, Czech Republic; petr.mosner@upce.cz (P.M.); ladislav.koudelka@upce.cz (L.K.)
  - <sup>3</sup> Department of Chemistry, Faculty of Science, University of Zagreb, Horvatovac 102a, 10000 Zagreb, Croatia; jana.pisk@chem.pmf.hr
  - <sup>4</sup> Department of Physics, Faculty of Science, University of Zagreb, Bijenička 32, 10000 Zagreb, Croatia
- \* Correspondence: zskoko@phy.hr (Ž.S.); lpavic@irb.hr (L.P.)

## 1. IR-ATR spectroscopy



**Citation:** Marijan, S.; Razum, M.; Sklepić Kerhač, K.; Mošner, P.; Koudelka, L.; Pisk, J.; Moguš-Milanković, A.; Skoko, Ž.; Pavić, L. Crystallization Behavior of Na<sub>2</sub>O-GeO<sub>2</sub>-P<sub>2</sub>O<sub>5</sub> Glass System: (Micro)Structural, Electrical, and Dielectric Study. *Materials* **2024**, *17*, 306. <https://doi.org/10.3390/ma17020306>

Academic Editor: Pengfei Wang

Received: 7 December 2023

Revised: 2 January 2024

Accepted: 5 January 2024

Published: 7 January 2024



**Copyright:** © 2024 by the authors. Licensee MDPI, Basel, Switzerland. This article is an open access article distributed under the terms and conditions of the Creative Commons Attribution (CC BY) license (<https://creativecommons.org/licenses/by/4.0/>).

**Figure S1.** (a) IR-ATR spectra of all samples from this study and (b) comparison of IR-ATR spectra of NGP@500 GC and NaPO<sub>3</sub>.

The IR-ATR spectrum of NGP glass, see Figure S1(a), exhibits distinct bands characteristic of metatraphosphate (Q<sup>2</sup>) glasses, and it also reveals indications of pyrophosphate units (Q<sup>1</sup>), which is consistent with the O/P ratio of 3.1 [1]. The intense band observed at 1275 cm<sup>-1</sup>, followed by shoulder at 1110 cm<sup>-1</sup> is indicative of the asymmetric and symmetric stretching of non-bridging oxygen atoms in Q<sup>2</sup> units, respectively [2,3], while the bands at 970 cm<sup>-1</sup> and 890 cm<sup>-1</sup> can be attributed to the asymmetric stretching vibrations of P–O–P groups in metaphosphate units, manifesting as chains, rings, and terminal groups [2,3]. Additionally, low intensity shoulders at 1150 cm<sup>-1</sup> and 1035 cm<sup>-1</sup> can be assigned to asymmetric and symmetric stretching of non-

bridging oxygen atoms in  $Q^1$  units, respectively, which presence in small quantities is in accordance with O/P ratio in studied glass. Furthermore, the symmetric stretching vibrations of P–O–P within  $Q^2$  and  $Q^1$  units are found in the range between 640–810  $\text{cm}^{-1}$  [2,3]. Moreover, the bands around  $\sim 460 \text{ cm}^{-1}$  and  $\sim 520 \text{ cm}^{-1}$  can be ascribed to the bending vibrations of P–O–P and  $\text{PO}_2$  units within the metaphosphate framework [2,3]. Notably, the IR-ATR spectroscopy results for the initial glass correlate well with prior Raman spectroscopy findings [1].

In contrast to the broad and diffuse bands observed in the spectrum of the initial glass, the spectra of the prepared glass-ceramics exhibit well-defined, sharp signals characteristic of crystalline materials. As the heat-treatment temperature is elevated from  $450^\circ\text{C}$  to  $550^\circ\text{C}$ , a notable transformation in the appearance of the spectra becomes apparent. The spectrum of NGP@450 glass-ceramic exhibits initial signs of crystallization and the presence of a glass matrix. In contrast, the spectra of NGP@500 and NGP@550 glass-ceramics display remarkable similarity, reflecting a notably advanced stage of crystallization. Here, it's noteworthy to highlight that the acquired IR-ATR spectra of GC samples, characterized by a substantial amount of  $\text{NaPO}_3$  crystal phase, exhibit a striking similarity to the results of the structural analysis of  $\text{NaPO}_3$  documented in [4]. Additionally, the strong agreement observed between the IR-ATR spectra of the prepared GCs and the IR spectrum of the  $\text{NaPO}_3$  crystal phase (SpectraBase®), see Figure S1(b), provides additional confirmation that  $\text{NaPO}_3$  is the predominant phase within the samples.

## 2. SEM-EDS analysis

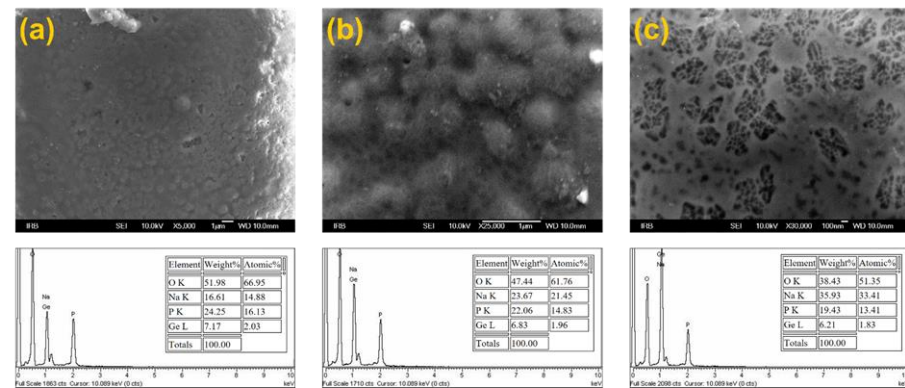


**Figure S2.** SEM images and EDS spectra of the NGP@450 glass-ceramic surface: (a) area, (b) surface – separation and (c) surface - separation 2.

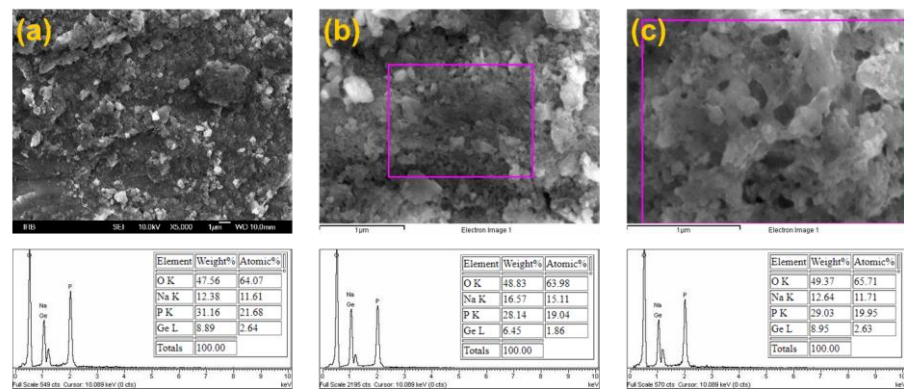


Figure S3. SEM images and EDS spectra of the NGP@500 glass-ceramic surface.

### 3. Electrical analysis

#### 3.1. Complex impedance plane– electrical equivalent circuit modelling

Table S1. Fitting parameters obtained from EEC modeling of complex impedance spectra measured at 150 °C for the initial glass and glass-ceramics from this study

Parameters	NGP	NGP@450	NGP@500	NGP@550
$R_1^a$ ( $\Omega$ )	$3.65 \times 10^5$	$3.06 \times 10^6$	$5.03 \times 10^7$	$1.96 \times 10^8$
$A_1^b$ ( $s^\alpha \Omega^{-1}$ )	$2.27 \times 10^{-11}$	$9.41 \times 10^{-12}$	$4.29 \times 10^{-11}$	$1.42 \times 10^{-11}$
$\alpha_1^c$	0.90	0.94	0.86	0.84
$C_1^d$ (F)	$6.22 \times 10^{-12}$	$4.92 \times 10^{-12}$	$1.50 \times 10^{-11}$	$4.63 \times 10^{-12}$
$R_2^a$ ( $\Omega$ )	-	$6.51 \times 10^6$	$3.59 \times 10^8$	$2.58 \times 10^8$
$A_2^b$ ( $s^\alpha \Omega^{-1}$ )	-	$9.23 \times 10^{-10}$	$6.56 \times 10^{-11}$	$2.09 \times 10^{-10}$
$\alpha_2^c$	-	0.60	0.71	0.66
$C_2^d$ (F)	-	$2.95 \times 10^{-11}$	$1.38 \times 10^{-11}$	$4.80 \times 10^{-11}$
$R_3^a$ ( $\Omega$ )	-	-	-	$4.12 \times 10^8$
$A_3^b$ ( $s^\alpha \Omega^{-1}$ )	-	-	-	$2.77 \times 10^{-9}$
$\alpha_3^c$	-	-	-	0.49
$C_3^d$ (F)	-	-	-	$3.18 \times 10^{-9}$
$A_4^b$ ( $s^\alpha \Omega^{-1}$ )	$8.85 \times 10^{-6}$	$2.81 \times 10^{-7}$	$2.37 \times 10^{-8}$	$7.16 \times 10^{-8}$
$\alpha_4^c$	0.91	0.67	0.40	0.81

<sup>a</sup> Individual resistance ( $R$ ) values for each R-CPE circuit element in the proposed model.

<sup>b</sup>  $A$  – a constant (CPE capacitance) derived from the empirical impedance function,  $Z_{CPE}^* = 1/A(i\omega)^\alpha$ , measured in  $s^\alpha \Omega^{-1}$  unit. <sup>c</sup>  $\alpha$  – a constant ( $0 \leq \alpha \leq 1$ ) determined from the empirical function,  $Z_{CPE}^* = 1/A(i\omega)^\alpha$ . When  $\alpha = 1$  (true capacitor), the unit becomes  $s \Omega^{-1} = F$ .

<sup>d</sup> Individual capacitance ( $C$ ) values calculated for each R-CPE circuit element in the proposed model using the formula  $C = A(\omega_{max})^{\alpha-1}$ .

## 4. Dielectric analysis

### 4.1. Complex Modulus Formalism

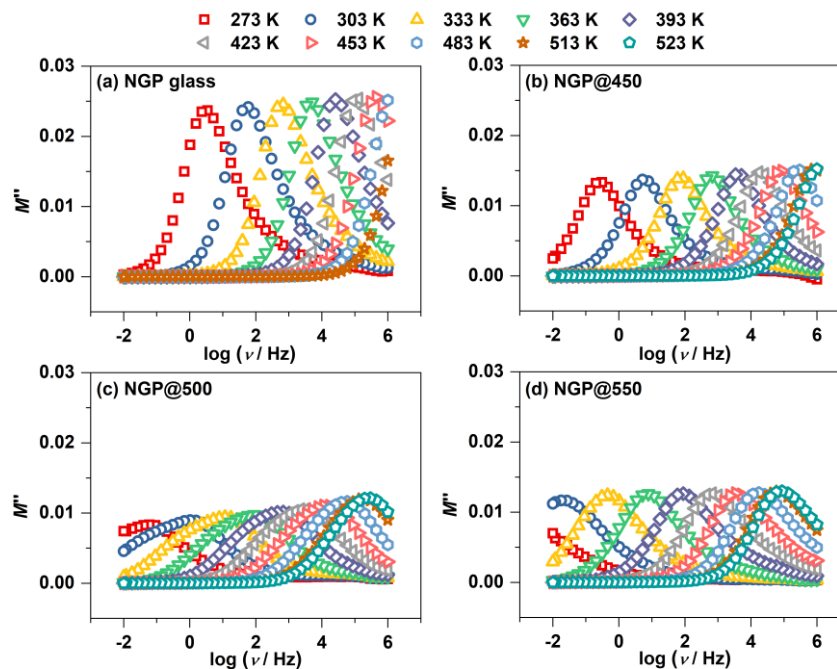


Figure S4. Spectra of imaginary moduli,  $M''(\omega)$ , for all samples.

## References

1. Sklepić, K.; Tricot, G.; Mošner, P.; Koudelka, L.; Moguš-Milanković, A. Sodium Ion Conductivity in Mixed Former  $\text{Na}_2\text{O}-\text{P}_2\text{O}_5-\text{GeO}_2$  and  $\text{Na}_2\text{O}-\text{B}_2\text{O}_3-\text{P}_2\text{O}_5-\text{GeO}_2$  Glasses. *J. Phys. Chem. C* **2021**, *125*, 10593–10604, doi:10.1021/acs.jpcc.1c00072.
2. Moustafa, Y.M.; El-Egili, K. Infrared Spectra of Sodium Phosphate Glasses. *J. Non-Cryst. Solids* **1998**, *240*, 144–153, doi:10.1016/S0022-3093(98)00711-X.
3. Sahar, M.R.; Hussein, A.W.M.A.; Hussin, R. Structural Characteristic of  $\text{Na}_2\text{O}-\text{P}_2\text{O}_5-\text{GeO}_2$  Glass Systems. *J. Non-Cryst. Solids* **2007**, *353*, 1134–1140, doi:10.1016/j.jnoncrysol.2006.12.032.
4. Trivedi, S.; Pamidi, V.; Fichtner, M.; Reddy, M.A. Ionically Conducting Inorganic Binders: A Paradigm Shift in Electrochemical Energy Storage. *Green Chem.* **2022**, *24*, 5620–5631, doi:10.1039/D2GC01389D.